

Articles

Luminescent Properties of Rare-Earth-Metal Ion-Doped KLaNb_2O_7 with Layered Perovskite Structures

Akihiko Kudo

Department of Applied Chemistry, Faculty of Science, Science University of Tokyo,
1-3 Kagurazaka, Shinjuku-ku, Tokyo 162, Japan

Received April 3, 1996. Revised Manuscript Received December 31, 1996⁸

Rare-earth-metal ions (Pr^{3+} , Sm^{3+} , Eu^{3+} , Tb^{3+} , Dy^{3+} , and Er^{3+}) doped in KLaNb_2O_7 with a layered perovskite structure showed photoluminescence by excitation of the two-dimensional host at 77 K. Dy^{3+} - and Er^{3+} -doped KLaNb_2O_7 showed the luminescence of both rare-earth-metal ions and host. In contrast, Pr^{3+} -, Sm^{3+} -, Eu^{3+} -, Tb^{3+} -doped KLaNb_2O_7 showed only the luminescence of their rare-earth-metal ions by host excitation, while the host luminescence was almost quenched. In the latter group, the characteristics of Tb^{3+} - and Pr^{3+} -doped KLaNb_2O_7 with respect to the temperature dependence of photoluminescence, afterglows and thermoluminescence were different from those of the others, suggesting that the hole-trapping process by the Tb^{3+} and Pr^{3+} played an important role for the characteristic behaviors. On the other hand, Sm^{3+} -doped KLaNb_2O_7 showed bright photoluminescence and thermoluminescence as a unique characteristic of the KLaNb_2O_7 system. In this process, Sm^{3+} ions in the perovskite layers seem to work as electron-trapping sites.

Introduction

Recently, the photophysical and photochemical properties of layered compounds have extensively been studied.¹ The photochemical properties of substances intercalated between the layers (interlayers) have mainly been investigated, while those of two-dimensional oxides of layered compounds have received little attention. Studying the photochemical properties of ion-exchangeable layered oxides consisting of titanium and niobium, for example, photocatalytic activities^{2–4} and luminescence,^{5–6} may provide a way to obtain new photoactive materials. Among the photochemical properties, the photochemical interaction between the hosts (the two-dimensional layers) and guests (the ions doped in the layers) is of particular interest. For example, Blasse et al. have investigated the luminescent properties of Eu^{3+} doped in NaLnTiO_4 in detail.⁷ They observed energy transfer from the TiO_6 units to Eu^{3+} . Toda et al. have reported the luminescent properties of Eu^{3+}

doped in a layered perovskite oxide ($\text{Na}_2\text{Gd}_2\text{Ti}_3\text{O}_{10}$).⁸ Thus, the luminescent properties of some two-dimensional titanates doped with rare-earth-metal ions have been reported, although most studies have dealt with only Eu^{3+} . The author has recently reported the luminescent properties of various rare-earth ions doped into $\text{K}_2\text{La}_2\text{Ti}_3\text{O}_{10}$.⁹ Niobates are also interesting photoactive host materials. Layered perovskite oxides (LPO) consisting of niobium, for example $\text{KC}_2\text{Nb}_3\text{O}_{10}$ ^{10,11} and KLaNb_2O_7 ,¹² have been synthesized as a niobate series. Their photocatalytic activities⁴ and luminescence⁵ have also been investigated. These LPOs are stable because they are stoichiometric oxides. Among them, KLaNb_2O_7 consists of perovskite layers (LaNb_2O_7) including La^{3+} and ion-exchangeable potassium ions at the interlayers.^{12,13} Therefore, the photochemical property of KLaNb_2O_7 as a two-dimensional host of lanthanide phosphors seems worthy of investigation.

In the present paper, the photoluminescence, afterglow, and thermoluminescence of KLaNb_2O_7 doped with various trivalent lanthanide metal ions (Pr^{3+} , Sm^{3+} , Eu^{3+} , Tb^{3+} , Dy^{3+} , and Er^{3+}) have been investigated. The luminescent properties of this system are also discussed in comparison with those of the $\text{K}_2\text{La}_2\text{Ti}_3\text{O}_{10}$ system

⁸ Abstract published in *Advance ACS Abstracts*, February 15, 1997.

(1) Ogawa, M.; Kuroda, K. *Chem. Rev. (Washington, D.C.)* **1995**, *95*, 399 and references therein.

(2) Shibata, M.; Kudo, A.; Tanaka, A.; Domen, K.; Maruya, K.; Onishi, T. *Chem. Lett.* **1987**, 1017.

(3) Domen, K.; Kudo, A.; Shinozaki, A.; Tanaka, A.; Maruya, K.; Onishi, T. *J. Chem. Soc., Chem. Commun.* **1986**, 356. Kudo, A.; Sayama, K.; Tanaka, A.; Asakura, A.; Domen, K.; Maruya, K.; Onishi, T. *J. Catal.* **1989**, *120*, 337.

(4) Domen, K.; Yoshimura, J.; Sekine, T.; Tanaka, A.; Onishi, T. *Catal. Lett.* **1990**, *4*, 339. Domen, K.; Ebina, Y.; Sekine, T.; Tanaka, A.; Kondo, J.; Hirose, C. *Catal. Today* **1993**, *16*, 479.

(5) Wiegel, M.; Hamoumi, M.; Blasse, G. *Mater. Chem. Phys.* **1994**, *36*, 289.

(6) Kudo, A.; Sakata, T. *J. Mater. Chem.* **1993**, *3*, 1081. Kudo, A.; Sakata, T. *Chem. Lett.* **1994**, 2179. Kudo, A.; Sakata, T. *J. Phys. Chem.* **1996**, *100*, 17323.

(7) Blasse, G.; Bril, A. *J. Chem. Phys.* **1968**, *48*, 3652. Berdowski, P. A. M.; Blasse, G. *J. Lumin.* **1984**, *29*, 243.

(8) Toda, K.; Sato, M. *J. Alloys Compound* **1995**, *218*, 228.

(9) Kudo, A.; Sakata, T. *J. Phys. Chem.* **1995**, *99*, 15963.

(10) Dion, M.; Ganne, M.; Tournoux, M. *Mater. Res. Bull.* **1981**, *16*, 1429. Dion, M.; Ganne, M.; Tournoux, M. *Rev. Chim. Miner.* **1984**, *21*, 92. Dion, M.; Ganne, M.; Tournoux, M. *Rev. Chim. Miner.* **1986**, *23*, 61.

(11) Jacobson, A. J.; Lewandowski, J. T.; Johnson, J. W. *J. Less-Common Met.* **1986**, *116*, 137. Jacobson, A. J.; Johnson, J. W.; Lewandowski, J. T. *Inorg. Chem.* **1985**, *24*, 3727. Jacobson, A. J.; Lewandowski, J. T.; Johnson, J. W. *Mater. Res. Bull.* **1990**, *25*, 679.

(12) Gopalakrishnan, J.; Bhat, V. *Mater. Res. Bull.* **1987**, *22*, 413.

(13) (a) Sato, M.; Abe, J.; Jin, T.; Ohta, M. *Solid State Ionics*, **1992**, *51*, 85. (b) Sato, M.; Toda, K.; Watanabe, J.; Uematsu, K. *Nippon Kagaku-kaishi* **1993**, 640.

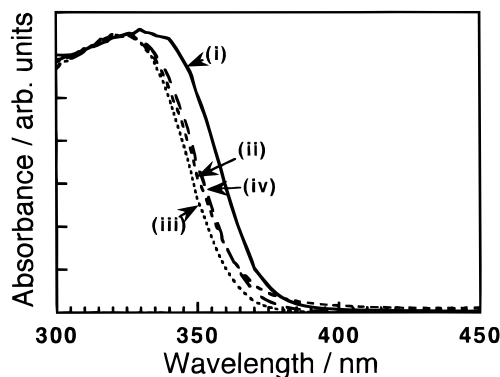


Figure 1. Diffuse reflection spectra of $\text{KLa}_{0.98}\text{Ln}_{0.02}\text{Nb}_2\text{O}_7$ at 300 K. (i) KLaNb_2O_7 , (ii) $\text{KLa}_{0.98}\text{Pr}_{0.02}\text{Nb}_2\text{O}_7$, (iii) $\text{KLa}_{0.98}\text{Sm}_{0.02}\text{Nb}_2\text{O}_7$, (iv) $\text{KLa}_{0.98}\text{Eu}_{0.02}\text{Nb}_2\text{O}_7$.

with a layered perovskite structure consisting of lanthanum–titanium oxides.

Experimental Section

The following reagents were used as starting materials: K_2CO_3 (Kanto Chemical, 99.5%), Nb_2O_5 (Wako Pure Chemical, 99.9%), La_2O_3 (Wako Pure Chemical, 99.99%), Pr_6O_{11} (Wako Pure Chemical, 99.5%), Sm_2O_3 (Wako Pure Chemical, 99.9%), Eu_2O_3 (Shin-etsu Chemical, 99.9%), Tb_4O_7 (Kanto Chemical, 99.95%), Dy_2O_3 (Shin-etsu Chemical, 99.9%), and Er_2O_3 (Wako Pure Chemical, 99.9%). KLaNb_2O_7 and KLaNb_2O_7 doped with rare-earth-metal ions of 2 mol % to La ($\text{KLa}_{0.98}\text{Ln}_{0.02}\text{Nb}_2\text{O}_7$) were prepared by calcination of the mixture of starting materials at 1423 K for 40 h, with one grinding between, after precalcination at 1173 K for 5 h in air using a platinum crucible.¹² X-ray diffraction patterns of Ln^{3+} - KLaNb_2O_7 were agreed with that of the native KLaNb_2O_7 and no extra XRD patterns due to the Ln oxides were observed, indicating that the materials obtained were single phases. The XRD data showed that all rare-earth metal ions of 2% should be homogeneously doped. The doped Ln^{3+} should be substituted in the La sites in KLaNb_2O_7 judging from the ion charges and the ionic radii. Sintered disks were used for undoped and Pr^{3+} -, Sm^{3+} -, and Tb^{3+} -doped KLaNb_2O_7 . Powdered samples were used for others. Luminescence of powdered or sintered disk samples was measured in a quartz glass cell or a cryostat with a temperature controller in vacuo using a fluorometer (Spex, Fluoromax). Diffuse reflection spectra were measured at room temperature using a UV–vis–NIR spectrometer (JASCO, Ubest V-570). The diffuse reflection spectra were converted to the absorbance mode by the Kubelka–Munk method.

Results

Diffuse Reflection Spectra. The diffuse reflection spectrum of native KLaNb_2O_7 has an onset at around 380 nm as shown in Figure 1. The spectra of $\text{KLa}_{0.98}\text{Ln}_{0.02}\text{Nb}_2\text{O}_7$ ($\text{Ln} = \text{Pr}, \text{Sm}, \text{and Eu}$) are blue-shifted (ca. 8 nm) compared with KLaNb_2O_7 , but their shapes are similar to each other. The blue-shift indicates that the energy structure of the perovskite layers can be controlled by replacing La^{3+} with other ions.

Photoluminescent Properties of Undoped and Rare-Earth Ion-Doped KLaNb_2O_7 . Figure 2a shows the photoluminescence spectra of native KLaNb_2O_7 (host) at 77 K. The broad emission is observed at around 600 nm. The excitation spectrum has an onset at around 380 nm corresponding to the diffuse reflection spectrum (Figure 1i). Blasse et al. have already reported the luminescent properties of perovskite-like niobates.⁵ The result obtained in the present study agrees with their results.

Figure 2b shows the photoluminescence spectra of $\text{KLa}_{0.98}\text{Pr}_{0.02}\text{Nb}_2\text{O}_7$ at 280 K. In the emission spectrum, the luminescence of Pr^{3+} ($^1\text{D}_2 \rightarrow ^3\text{H}_4$) is observed by the excitation at 368 nm. In the excitation spectrum, besides sharp peaks due to the direct excitation of Pr^{3+} ions (449.5 nm), a broad band is observed at 370 nm. This broad band is considerably different from the diffuse reflection spectrum (Figure 1ii) and the excitation spectrum of native KLaNb_2O_7 (Figure 2a). This suggests that there are two kinds of absorption bands. At least one resulted in luminescence but the other did not at 280 K. At 77 K, the host luminescence is completely quenched and only the luminescence of Pr^{3+} is observed by the host excitation (340 nm) as shown in Figure 2c. The excitation spectrum at 77 K has a similar shape to that of native KLaNb_2O_7 (Figure 2a) being different from that at 280 K. It is noteworthy that the intensity ratio of the emission peak at 608 nm ($^1\text{D}_2 \rightarrow ^3\text{H}_4$) to those at 490, 550, 620, and 650 nm ($^3\text{P}_0 \rightarrow ^3\text{H}_4$, $^5, 6$ and $^3\text{F}_2$, respectively) by the host excitation (ii in Figure 2c) is considerably larger than that by direct excitation of Pr^{3+} ions (iii in Figure 2c). Thus, it was found that the luminescence intensity ratios between different energy modes by host excitation were different from those by direct excitation of Pr^{3+} ions.

Figure 2d shows the photoluminescence spectra of $\text{KLa}_{0.98}\text{Sm}_{0.02}\text{Nb}_2\text{O}_7$ at 77 K. The luminescence of Sm^{3+} ($^4\text{G}_{5/2} \rightarrow ^6\text{H}_{5/2, 7/2, 9/2}$) is observed by the host excitation as well as the luminescence by the direct excitation of the Sm^{3+} ions. The host luminescence is completely quenched. At 300 K, the luminescence was observed only by the direct excitation of Sm^{3+} ions but not by the host excitation.

Figure 2e shows the photoluminescence spectra of $\text{KLa}_{0.98}\text{Eu}_{0.02}\text{Nb}_2\text{O}_7$ at 300 K. The luminescence of Eu^{3+} ($^5\text{D}_0 \rightarrow ^7\text{F}_{0,1,2,3,4}$) was observed by the excitation at 370 nm. The excitation spectrum does not fit to the diffuse reflection spectrum (Figure 1iv) as well as in the case of $\text{KLa}_{0.98}\text{Pr}_{0.02}\text{Nb}_2\text{O}_7$ at 280 K (Figure 2b). The band around 370 nm in the excitation spectrum might be due to the charge transfer.⁷ The similar band was also observed for a Eu^{3+} -doped $\text{K}_2\text{La}_2\text{Ti}_3\text{O}_{10}$ system.⁹ At 77 K, the luminescence of Eu^{3+} is observed by the host excitation at 340 nm, while the host luminescence is not observed as shown in Figure 2f. In the excitation spectrum, the band by the host excitation is much smaller than those by the direct excitation of Eu^{3+} ions at 77 K. Both at 300 and at 77 K, the luminescence intensity due to the $^5\text{D}_0 \rightarrow ^7\text{F}_0$ transition by the host excitation is relatively larger than that by the direct excitation of Eu^{3+} ions (compare ii with iii in Figure 2e,f).

Figure 2g shows the photoluminescence spectra of $\text{KLa}_{0.98}\text{Tb}_{0.02}\text{Nb}_2\text{O}_7$ at 77 K. The host luminescence is quenched, and only the luminescence of Tb^{3+} ($^5\text{D}_4 \rightarrow ^7\text{F}_{4,5,6}$) is observed by the host excitation. In the excitation spectrum, small peaks at 368 and 377 nm are observed due to the direct excitation of Tb^{3+} ions. However, these intensities are much lower than that of the host excitation band as well as observed in $\text{KLa}_{0.98}\text{Pr}_{0.02}\text{Nb}_2\text{O}_7$ (Figure 2c), suggesting that energy transfer from the host to Pr^{3+} and Tb^{3+} occurs with high efficiencies. At 300 K, however, the luminescence of Tb^{3+} by the host excitation was not observed.

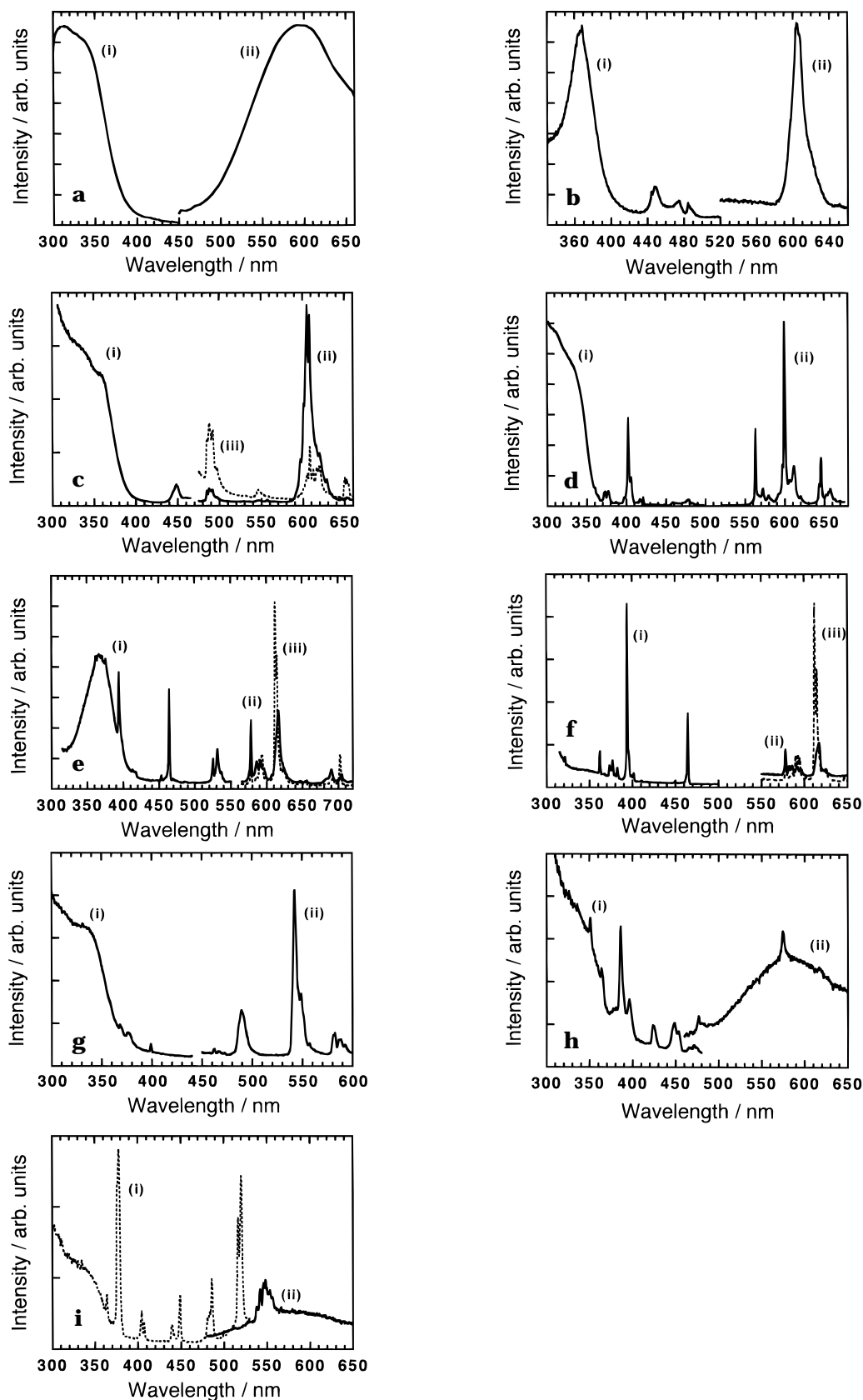


Figure 2. Photoluminescence spectra of $\text{KLa}_{0.98}\text{Ln}_{0.02}\text{Nb}_2\text{O}_7$. (a) KLaNb_2O_7 , (i) excitation (monitored at 590 nm) and (ii) emission (excited at 345 nm) spectra at 77 K. (b) $\text{KLa}_{0.98}\text{Pr}_{0.02}\text{Nb}_2\text{O}_7$, (i) excitation (monitored at 605 nm) and (ii) emission (excited at 368 nm) spectra at 280 K. (c) $\text{KLa}_{0.98}\text{Pr}_{0.02}\text{Nb}_2\text{O}_7$, (i) excitation (monitored at 608 nm), (ii) emission (excited at 340 nm), and (iii) emission (excited at 449.5 nm) spectra at 77 K. (d) $\text{KLa}_{0.98}\text{Sm}_{0.02}\text{Nb}_2\text{O}_7$, (i) excitation (monitored at 599.5 nm) and (ii) emission (excited at 340 nm) spectra at 77 K. (e) $\text{KLa}_{0.98}\text{Eu}_{0.02}\text{Nb}_2\text{O}_7$, (i) excitation (monitored at 616.5 nm), (ii) emission (excited at 370 nm), and (iii) emission (excited at 394 nm) spectra at 300 K. (f) $\text{KLa}_{0.98}\text{Eu}_{0.02}\text{Nb}_2\text{O}_7$, (i) excitation (monitored at 612 nm), (ii) emission (excited at 355 nm), and (iii) emission (excited at 394 nm) spectra at 77 K. (g) $\text{KLa}_{0.98}\text{Tb}_{0.02}\text{Nb}_2\text{O}_7$, (i) excitation (monitored at 542 nm) and (ii) emission (excited at 340 nm) spectra at 77 K. (h) $\text{KLa}_{0.98}\text{Dy}_{0.02}\text{Nb}_2\text{O}_7$, (i) excitation (monitored at 576 nm) and (ii) emission (excited at 350 nm) spectra at 77 K. (i) $\text{KLa}_{0.98}\text{Er}_{0.02}\text{Nb}_2\text{O}_7$, (i) excitation (monitored at 548 nm) and (ii) emission (excited at 345 nm) spectra at 77 K.

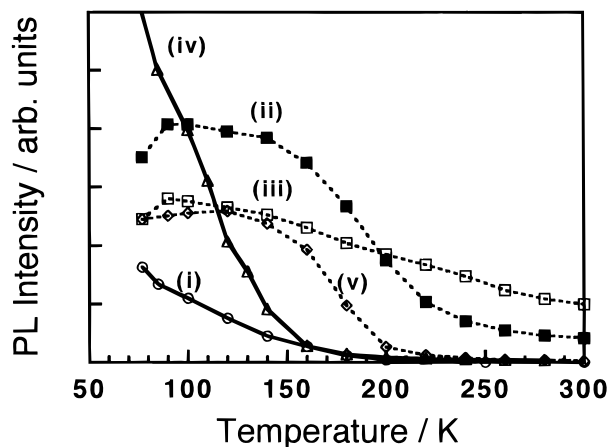


Figure 3. Temperature dependence of photoluminescence intensity of $\text{KLa}_{0.98}\text{Ln}_{0.02}\text{Nb}_2\text{O}_7$ ($\text{Ln} = \text{La}, \text{Pr}, \text{Sm}, \text{and Tb}$). (i) KLaNb_2O_7 ; excited at 345 nm, monitored at 590 nm. (ii) $\text{KLa}_{0.98}\text{Pr}_{0.02}\text{Nb}_2\text{O}_7$; excited at 340 nm, monitored at 608 nm. (iii) $\text{KLa}_{0.98}\text{Pr}_{0.02}\text{Nb}_2\text{O}_7$; excited at 449.5 nm, monitored at 608 nm. (iv) $\text{KLa}_{0.98}\text{Sm}_{0.02}\text{Nb}_2\text{O}_7$; excited at 340 nm, monitored at 599.5 nm. (v) $\text{KLa}_{0.98}\text{Tb}_{0.02}\text{Nb}_2\text{O}_7$; excited at 340 nm, monitored at 542 nm.

Figure 2h,i shows the photoluminescence spectra of $\text{KLa}_{0.98}\text{Dy}_{0.02}\text{Nb}_2\text{O}_7$ and $\text{KLa}_{0.98}\text{Er}_{0.02}\text{Nb}_2\text{O}_7$ at 77 K, respectively. The luminescence of Dy^{3+} ($^4\text{F}_{9/2,11/2} \rightarrow ^6\text{H}_{15/2}$) and Er^{3+} ($^4\text{S}_{3/2} \rightarrow ^4\text{I}_{15/2}$) is observed by the host excitation. However, in these cases, the broad luminescence of the host remained. The quenching of the host luminescence for $\text{KLa}_{0.98}\text{Er}_{0.02}\text{Nb}_2\text{O}_7$ seems larger than that for $\text{KLa}_{0.98}\text{Dy}_{0.02}\text{Nb}_2\text{O}_7$. Resonance energy transfer can contribute to the quenching of the host luminescence as well as energy transfer by electron and hole carriers. The excitation spectrum of Er^{3+} , for example at 520 nm, largely overlaps with the host emission spectrum, while that of Dy^{3+} does not so. Therefore, the resonance energy transfer for $\text{KLa}_{0.98}\text{Er}_{0.02}\text{Nb}_2\text{O}_7$ would occur more easily than that for $\text{KLa}_{0.98}\text{Dy}_{0.02}\text{Nb}_2\text{O}_7$. At 300 K, the luminescence of Dy^{3+} and Er^{3+} was observed only by the direct excitation of their ions.

In summary, Pr^{3+} , Sm^{3+} , Eu^{3+} , and Tb^{3+} -doped KLaNb_2O_7 showed only the luminescence of their rare-earth-metal ions by the host excitation at 77 K accompanied with complete quenching of host luminescence. In contrast, Dy^{3+} and Er^{3+} -doped KLaNb_2O_7 showed both their rare-earth-metal ions and the host luminescence. If undoped materials had existed, the host luminescence should not be completely quenched. However, the host emission was almost completely quenched for the Pr^{3+} , Sm^{3+} , Eu^{3+} , and Tb^{3+} -doped materials. This result indicates that the ions should be doped in the host. One might think that the remains of the host luminescence in the cases of $\text{KLa}_{0.98}\text{Er}_{0.02}\text{Nb}_2\text{O}_7$ and $\text{KLa}_{0.98}\text{Dy}_{0.02}\text{Nb}_2\text{O}_7$ would be due to the undoped impurities. However, the XRD data can deny it.

Luminescent Properties of $\text{KLa}_{0.98}\text{Ln}_{0.02}\text{Nb}_2\text{O}_7$ ($\text{Ln} = \text{La}, \text{Pr}, \text{Sm}, \text{and Tb}$). Figure 3 shows the temperature dependence of the photoluminescence (PL) intensity. The PL intensities of KLaNb_2O_7 and $\text{KLa}_{0.98}\text{Sm}_{0.02}\text{Nb}_2\text{O}_7$ are increased by lowering the temperature below 180 K. In contrast, the PL intensities of $\text{KLa}_{0.98}\text{Pr}_{0.02}\text{Nb}_2\text{O}_7$ and $\text{KLa}_{0.98}\text{Tb}_{0.02}\text{Nb}_2\text{O}_7$ arise at higher temperature (200–250 K) and saturate at around 120

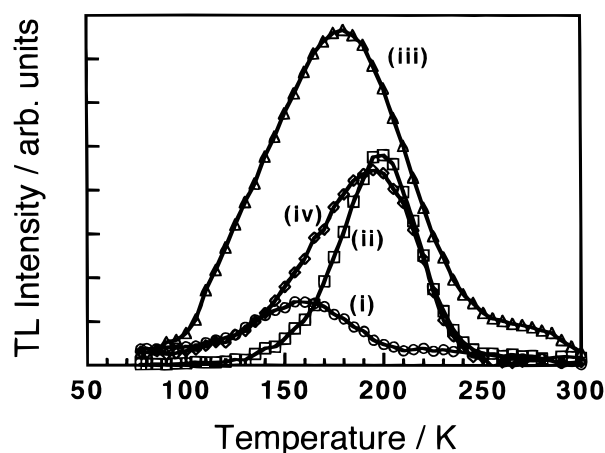


Figure 4. Glow curves of $\text{KLa}_{0.98}\text{Ln}_{0.02}\text{Nb}_2\text{O}_7$ ($\text{Ln} = \text{La}, \text{Pr}, \text{Sm}, \text{and Tb}$). (i) KLaNb_2O_7 ; monitored at 590 nm. (ii) $\text{KLa}_{0.98}\text{Pr}_{0.02}\text{Nb}_2\text{O}_7$; monitored at 605 nm. (iii) $\text{KLa}_{0.98}\text{Sm}_{0.02}\text{Nb}_2\text{O}_7$; monitored at 599.5 nm. (iv) $\text{KLa}_{0.98}\text{Tb}_{0.02}\text{Nb}_2\text{O}_7$; monitored at 542.5 nm.

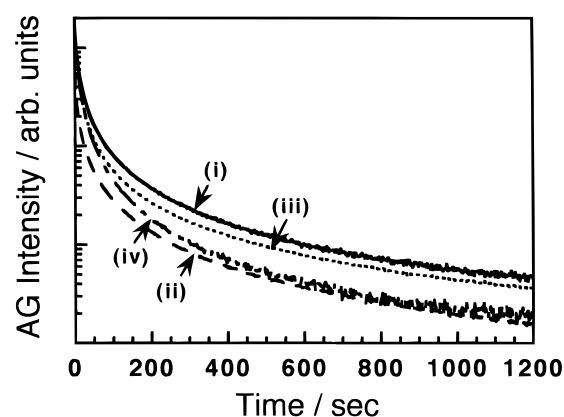


Figure 5. Afterglows of $\text{KLa}_{0.98}\text{Ln}_{0.02}\text{Nb}_2\text{O}_7$ ($\text{Ln} = \text{La}, \text{Pr}, \text{Sm}, \text{and Tb}$). (i) KLaNb_2O_7 ; monitored at 590 nm. (ii) $\text{KLa}_{0.98}\text{Pr}_{0.02}\text{Nb}_2\text{O}_7$; monitored at 605 nm. (iii) $\text{KLa}_{0.98}\text{Sm}_{0.02}\text{Nb}_2\text{O}_7$; monitored at 599.5 nm. (iv) $\text{KLa}_{0.98}\text{Tb}_{0.02}\text{Nb}_2\text{O}_7$; monitored at 542.5 nm.

K. The PL intensity of $\text{KLa}_{0.98}\text{Pr}_{0.02}\text{Nb}_2\text{O}_7$ by the host excitation strongly depends on the temperature (Figure 3ii) while that by the direct excitation of Pr^{3+} ions does not vary as much (Figure 3iii).

Figure 4 shows glow curves which were obtained by monitoring the thermoluminescence (TL) of the host for KLaNb_2O_7 and of rare-earth ions for $\text{KLa}_{0.98}\text{Pr}_{0.02}\text{Nb}_2\text{O}_7$, $\text{KLa}_{0.98}\text{Sm}_{0.02}\text{Nb}_2\text{O}_7$, and $\text{KLa}_{0.98}\text{Tb}_{0.02}\text{Nb}_2\text{O}_7$. The TL was observed only by the host excitation, suggesting that trap processes in the host lattice took part in the TL. Glow curves of Pr^{3+} , Sm^{3+} , and Tb^{3+} -doped KLaNb_2O_7 shift to higher temperature side compared with that of native KLaNb_2O_7 . The shift is especially large in the cases of $\text{KLa}_{0.98}\text{Pr}_{0.02}\text{Nb}_2\text{O}_7$ and $\text{KLa}_{0.98}\text{Tb}_{0.02}\text{Nb}_2\text{O}_7$. The maximums of TL intensity for $\text{KLa}_{0.98}\text{Pr}_{0.02}\text{Nb}_2\text{O}_7$ and $\text{KLa}_{0.98}\text{Tb}_{0.02}\text{Nb}_2\text{O}_7$ are around 200 K where KLaNb_2O_7 does not show luminescence as shown in Figure 3.

$\text{KLa}_{0.98}\text{Ln}_{0.02}\text{Nb}_2\text{O}_7$ ($\text{Ln} = \text{La}, \text{Pr}, \text{Sm}, \text{and Tb}$) shows long afterglows (AG > 20 min) as shown in Figure 5. These AGs were measured by monitoring the luminescence of the host for KLaNb_2O_7 and of rare-earth ions for $\text{KLa}_{0.98}\text{Pr}_{0.02}\text{Nb}_2\text{O}_7$, $\text{KLa}_{0.98}\text{Sm}_{0.02}\text{Nb}_2\text{O}_7$, and $\text{KLa}_{0.98}\text{Tb}_{0.02}\text{Nb}_2\text{O}_7$ after exciting their hosts for 5 min. These AGs were observed only by the host excitation but not

by direct excitation of ions suggesting that trapping processes in the host were important as well as observed in TL. The decays of these AGs of $\text{KLa}_{0.98}\text{Pr}_{0.02}\text{Nb}_2\text{O}_7$ and $\text{KLa}_{0.98}\text{Tb}_{0.02}\text{Nb}_2\text{O}_7$ are faster than those of KLaNb_2O_7 and $\text{KLa}_{0.98}\text{Sm}_{0.02}\text{Nb}_2\text{O}_7$.

Discussion

Blasse et al. have discussed the luminescent properties of perovskite-like titanates and niobates in detail.⁵ The angles of the M–O–M bonds are important for delocalization of the excited states in both titanates and niobates. Let us see the structures of KLaNb_2O_7 and $\text{K}_2\text{La}_2\text{Ti}_3\text{O}_{10}$. Both KLaNb_2O_7 and $\text{K}_2\text{La}_2\text{Ti}_3\text{O}_{10}$ have layered perovskite structures. KLaNb_2O_7 consists of double perovskite slabs of lanthanum niobate and have distorted NbO_6 units with short Nb–O bonds (1.695 Å) which stick out into the interlayer region.^{12,13a} $\text{K}_2\text{La}_2\text{Ti}_3\text{O}_{10}$ has three-octahedra-thick perovskite slabs of lanthanum titanate.¹⁴ The TiO_6 units in the middle layers of the triple-perovskite slabs in $\text{K}_2\text{La}_2\text{Ti}_3\text{O}_{10}$ are not distorted very much, while those of the layers facing the interlayers are largely distorted, resulting in short Ti–O bonds (1.719 Å).^{13b} At the middle layers, the angle of Ti–O–Ti bonds should be close to 180°. An excited state in $\text{K}_2\text{La}_2\text{Ti}_3\text{O}_{10}$ seems to be delocalized more than that in KLaNb_2O_7 , judging from the number of thicknesses of perovskite slabs and the M–O–M bond angles. Therefore, it is important to compare the luminescent properties of Ln^{3+} -doped KLaNb_2O_7 with those of Ln^{3+} -doped $\text{K}_2\text{La}_2\text{Ti}_3\text{O}_{10}$.

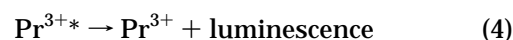
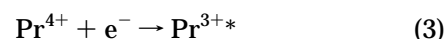
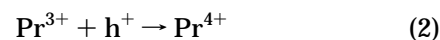
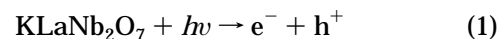
In the native KLaNb_2O_7 and $\text{K}_2\text{La}_2\text{Ti}_3\text{O}_{10}$, the onsets of the excitation and diffuse reflection spectra and the maximum of the emission band are located at longer wavelength in KLaNb_2O_7 in comparison with those in $\text{K}_2\text{La}_2\text{Ti}_3\text{O}_{10}$ (the onset of the excitation spectrum; 330 nm, the maximum of emission spectrum; 475 nm).⁹ Moreover, the Stokes shifts of KLaNb_2O_7 and $\text{K}_2\text{La}_2\text{Ti}_3\text{O}_{10}$ are 14 000 and 10 500 cm^{-1} , respectively. These shifts are due to the different energy levels between the perovskite oxide layers consisting of NbO_6 and TiO_6 units and the degree of delocalization.

The luminescence from the $^3\text{P}_0$ level of Pr^{3+} in $\text{KLa}_{0.98}\text{Pr}_{0.02}\text{Nb}_2\text{O}_7$ was less efficient than that from $^1\text{D}_2$. Here, the excitation energy of a Pr^{3+} ion to its $^3\text{P}_0$ level is higher than that to $^1\text{D}_2$. In contrast, in the case of $\text{K}_2\text{La}_{1.98}\text{Pr}_{0.02}\text{Ti}_3\text{O}_{10}$, the luminescence from the $^3\text{P}_0$ level was predominant. These results would also reflect the energy difference between KLaNb_2O_7 and $\text{K}_2\text{La}_2\text{Ti}_3\text{O}_{10}$ systems. Namely, the emission energy of $\text{K}_2\text{La}_2\text{Ti}_3\text{O}_{10}$ is sufficient for exciting Pr^{3+} to its $^3\text{P}_0$ level, while that of KLaNb_2O_7 is not so. This is clear from the energies of their emission spectra.

In the $\text{KLa}_{0.98}\text{Pr}_{0.02}\text{Nb}_2\text{O}_7$ system, the intensity ratio of the emission from a $^3\text{P}_0$ level to the emission from a $^1\text{D}_2$ level by host excitation was smaller than that by direct excitation (449.5 nm) as shown in Figure 2c. This indicates that the transition to the $^3\text{P}_0$ level by energy transfer from the host is disadvantageous compared with that to the $^1\text{D}_2$ because the excitation energy from the host is smaller than the direct excitation energy. Also in the $\text{KLa}_{0.98}\text{Eu}_{0.02}\text{Nb}_2\text{O}_7$ system, the luminescence intensity due to the $^5\text{D}_0 \rightarrow ^7\text{F}_0$ transition by the host excitation is relatively larger than that by the direct

excitation of Eu^{3+} ions as shown in Figure 2e,h. However, the reason for the behavior $\text{KLa}_{0.98}\text{Eu}_{0.02}\text{Nb}_2\text{O}_7$ is not clear at the present stage. It should be noted that, in a NaLnTiO_4 system, such a change in the relative intensity of $^5\text{D}_0 \rightarrow ^7\text{F}_J$ transitions depended on a kind of Ln.⁷

The host luminescence remained in KLaNb_2O_7 doped with Dy^{3+} and Er^{3+} while it was quenched in KLaNb_2O_7 doped with Pr^{3+} , Sm^{3+} , Eu^{3+} , and Tb^{3+} . This result is the same as that in the $\text{K}_2\text{La}_2\text{Ti}_3\text{O}_{10}$ system except for the Sm^{3+} -doped material. One remarkable characteristic property of the KLaNb_2O_7 system is that Sm^{3+} -doped KLaNb_2O_7 shows efficient luminescence at 77 K by the host excitation accompanied by the quenching of the host luminescence (Figures 2d and 3iv) and thermoluminescence (Figure 4iii). The characteristics of $\text{KLa}_{0.98}\text{Pr}_{0.02}\text{Nb}_2\text{O}_7$ and $\text{KLa}_{0.98}\text{Tb}_{0.02}\text{Nb}_2\text{O}_7$ for the luminescent properties were different from those of KLaNb_2O_7 and $\text{KLa}_{0.98}\text{Sm}_{0.02}\text{Nb}_2\text{O}_7$, namely, the photoluminescence and the maximums of the glow curves were observed at higher temperatures, and the lifetimes of the afterglow were shorter. These tendencies of the KLaNb_2O_7 system were the same as those of the $\text{K}_2\text{La}_2\text{Ti}_3\text{O}_{10}$ system. The fact that Pr^{3+} and Tb^{3+} can easily be tetravalent in oxides probably is responsible for the similar characteristics between $\text{KLa}_{0.98}\text{Pr}_{0.02}\text{Nb}_2\text{O}_7$ and $\text{KLa}_{0.98}\text{Tb}_{0.02}\text{Nb}_2\text{O}_7$. Accordingly, the hole trap process plays an important role in the luminescent properties of Pr^{3+} - and Tb^{3+} -doped KLaNb_2O_7 as well as in the $\text{K}_2\text{La}_2\text{Ti}_3\text{O}_{10}$ system.



This mechanism has been discussed in the previous paper.⁹ However, at 300 K, the luminescence of Pr^{3+} and Tb^{3+} in $\text{KLa}_{0.98}\text{Pr}_{0.02}\text{Nb}_2\text{O}_7$ and $\text{KLa}_{0.98}\text{Tb}_{0.02}\text{Nb}_2\text{O}_7$ was not observed by the host excitation while it was so in the case of the $\text{K}_2\text{La}_2\text{Ti}_3\text{O}_{10}$ system. This suggests that nonradiative transitions in the KLaNb_2O_7 system occur more easily than that in the $\text{K}_2\text{La}_2\text{Ti}_3\text{O}_{10}$ system. Higher delocalization in $\text{K}_2\text{La}_2\text{Ti}_3\text{O}_{10}$ than in KLaNb_2O_7 could assist in the hole-trapping process by Pr^{3+} and Tb^{3+} .

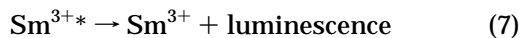
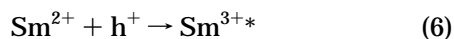
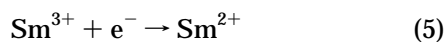
The host luminescence was quenched in $\text{KLa}_{0.98}\text{Eu}_{0.02}\text{Nb}_2\text{O}_7$ and $\text{KLa}_{0.98}\text{Sm}_{0.02}\text{Nb}_2\text{O}_7$ at 77 K. Moreover, efficient luminescence of $\text{KLa}_{0.98}\text{Sm}_{0.02}\text{Nb}_2\text{O}_7$ was observed by host excitation. Eu^{3+} and Sm^{3+} can become divalent more easily than other lanthanide trivalent ions. Mechanisms of electron trapping by Sm^{3+} and Eu^{3+} have been proposed, for example, in the luminescence of $\text{Lu}_{2-x}\text{YSiO}_5:\text{Ce}_y\text{Sm}_{0.001}$ of an X-ray storage phosphor¹⁵ and $\text{Y}_3\text{Al}_5\text{O}_{12}$ (YAG).¹⁶ The following mechanism accompanied with the electron-trapping process

(15) Meiss, D.; Reichardt, J.; Wischert, W.; Kemmler-Sack, S. *Phys. Status Solidi A* **1994**, *142*, 237.

(16) Robbins, D. J.; Cockayne, B.; Glasper, J. L.; Lent, B. J. *Electrochem. Soc.* **1979**, *126*, 1221.

(14) Gopalakrishnan, J.; Bhat, V. *Inorg. Chem.* **1987**, *26*, 4299.

could be applied to $\text{KLa}_{0.98}\text{Eu}_{0.02}\text{Nb}_2\text{O}_7$ and $\text{KLa}_{0.98}\text{Sm}_{0.02}\text{Nb}_2\text{O}_7$:



It was thought that the host luminescence was quenched by this process. In the cases of $\text{KLa}_{0.98}\text{Er}_{0.02}\text{Nb}_2\text{O}_7$ and $\text{KLa}_{0.98}\text{Dy}_{0.02}\text{Nb}_2\text{O}_7$, the host luminescence remained, indicating that the efficiencies of the energy transfer were not high. It is probably due to the lack of the electron-hole trapping process because the redox of these ions cannot occur easily. The major process is the resonant energy transfer in these cases.

Conclusions

Rare-earth ions (Pr^{3+} , Sm^{3+} , Eu^{3+} , Tb^{3+} , Dy^{3+} , and Er^{3+}) doped in KLaNb_2O_7 showed luminescence by host excitation at 77 K, indicating that excited states were delocalized in the lanthanum niobate perovskite layers.

The host luminescence was completely quenched in Pr^{3+} -, Sm^{3+} -, Eu^{3+} -, and Tb^{3+} -doped KLaNb_2O_7 probably by an electron- and hole-trapping process at their rare-earth ions.

The behaviors of $\text{KLa}_{0.98}\text{Pr}_{0.02}\text{Nb}_2\text{O}_7$ and $\text{KLa}_{0.98}\text{Tb}_{0.02}\text{Nb}_2\text{O}_7$ in the temperature dependence of photoluminescence, thermoluminescence, and afterglows were different from those of $\text{KLa}_{0.98}\text{Sm}_{0.02}\text{Nb}_2\text{O}_7$ and KLaNb_2O_7 as well as in the case of the $\text{K}_2\text{La}_2\text{Ti}_3\text{O}_{10}$ system.

In Pr^{3+} - and Eu^{3+} -doped KLaNb_2O_7 , the diffuse reflection spectra were different from the excitation spectra near room temperature, suggesting that there were two kinds of absorption bands: one resulted in luminescence but the other did not. The former might be due to the charge-transfer band.

In Pr^{3+} - and Eu^{3+} -doped KLaNb_2O_7 , the luminescence intensity ratios between different energy modes by host excitation were different from those by direct excitation of rare-earth ions.

$\text{KLa}_{0.8}\text{Sm}_{0.2}\text{Nb}_2\text{O}_7$ showed bright photoluminescence and thermoluminescence.

Acknowledgment. Support by Tokuyama Science Foundation and by Grants-in-Aid for Scientific Research (07740543) from the Ministry of Education, Science, and Culture is gratefully acknowledged.

CM9602149